

# Springback and Formability Studies on Friction Stir Welded Sheets

Sudhindra Katre, Siddhartha Karidi, B. Durga Rao,  
P. Janaki Ramulu and R. Ganesh Narayanan

**Abstract** In the present work, the effect of selected welding conditions on the temperature evolution, springback behaviour and formability of friction-stir welding (FSW) sheets is investigated. The Al6061T6-Al6061T6 combination is used for temperature evolution studies, while dissimilar Al combination made of Al6061T6 and Al5052H32 is used in springback and formability tests. The springback experiments are performed with a V-bending set-up without tension, and formability experiments are conducted using a limiting dome height (LDH) set-up. By increasing the shoulder diameter, plunge depth and tool rotation speed, the peak temperature is increased, and it is vice versa for welding speed. In the case of springback, the performance of FSW sheets is in between that of Al6061T6 and Al5052H32 base materials. Reduction in springback of FSW sheets is observed at higher rotational speed and welding speed, and this is correlating well with the modifications in tensile properties such as yield strength to elastic modulus ratio and strain hardening exponent of the weld zone (WZ) with varying FSW conditions. Three different modes of failures, normal and parallel to the WZ, are observed during formability testing of FSW sheets made of dissimilar Al grades at two different strain-paths. It is better to evaluate the forming limit of FSW sheets at individual strain-paths, rather than in all the strain-paths using a forming limit curve (FLC), because of changing failure pattern with changing strain-paths.

**Keywords** Friction-stir welding · Springback · Formability · Aluminium alloys · Forming limit

---

S. Katre · S. Karidi · R.G. Narayanan (✉)  
Department of Mechanical Engineering, IIT Guwahati, Guwahati 781039, India  
e-mail: ganu@iitg.ernet.in

B. Durga Rao  
Parala Maharaja Engineering College, Sitalapalli, Berhampur 761003, Orissa, India

P.J. Ramulu  
Department of Mechanical Engineering, Vardhaman College of Engineering, Kacheram,  
Shamshabad 501218, Hyderabad, India

## 1 Introduction

Friction-stir welding (FSW) is a solid-state joining process. It involves joining of metals without filler materials. A constantly rotating cylindrical-shouldered tool with a profiled nib is transversely fed at a constant rate into a butt joint between two clamped sheets (Fig. 1). Frictional heat is generated between the wear-resistant welding components and the work pieces. This heat, along with that generated by the mechanical mixing process and the adiabatic heat within the material, cause the stirred materials to soften without melting. Hence, this is called as a solid-state welding process. The resultant plasticized material is transferred from the leading edge of the tool to the trailing edge of the tool probe and is forged together by the intimate contact of the tool shoulder and the pin profile (Mishra and Ma 2005). There are many advantages of FSW including energy savings, exclusion of consumables and shielding gases, good dimensional stability, low distortion of work sheet, enriched metallurgical properties in the weld region, fine microstructure, possibility of welding dissimilar materials and reduced usage of fasteners for joining multiple parts. It is considered as ‘green technology’ because of the environmental friendliness and energy efficiency.

The important parameters in FSW are tool material and its geometry (both pin and shoulder), welding speed, tool rotational speed, axial force and work piece material quality. An appropriate combination of these parameters determines the excellence of welds including the presence of defects and microstructure and hence as a consequence the mechanical properties and formability of FSW sheets gets affected. The remaining part of the section describes some of the available work performed on springback and formability of unwelded and welded sheets.

During sheet bending, while one side of the sheet metal is subjected to compressive stress, the other surface is subjected to tensile stress. Once the load is released by withdrawal of the punch, an elastic recovery occurs because of the release of the elastic stresses in the bending process. This elastic recovery is called

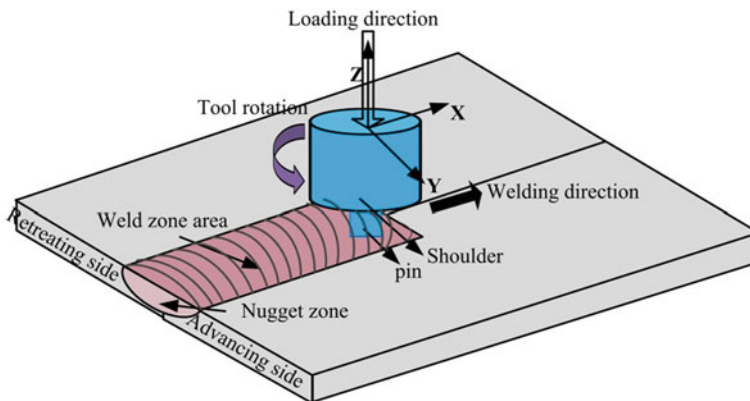


**Fig. 1** Schematic of friction-stir welding process

Springback. It is seen as a practical problem to predict the final geometry of the part accurately, after springback, and to design appropriate tooling for compensation. Overbending, bottoming and stretch bending are common methods of controlling springback. There are other methods, such as heat treating the materials, change in working temperature of material and tools, appropriate tool design, tool geometry design and recently the friction-stir processing/welding, that are used for springback control of sheets. It is shown by Moon et al. (2003) that the hot die and cold punch combination can reduce the springback of Al 1050 sheet up to 20 % when compared to conventional bending done at room temperature. The ram speed was also shown to have significant effect on controlling springback. Garcia-Romeu et al. (2007) have shown through experiments that sheet materials, their thicknesses and die widths affect the springback behaviour in a compounding fashion. It has been concluded by them that though small radius is preferred for springback, large radius dies are preferred in consideration of mechanical properties of bent part. Hence, one should optimize various factors governing the springback of sheets. Alves de Sousa et al. (2008) investigated the unconstrained springback of Al–Mg–Si sheets, by considering pre-strain before the actual deformation and later subjected to different sitting times at normal temperatures show that extensive amount of stress is relaxed when the punch is totally released. It is also observed that the springback angle decreases as the sitting time increases.

It is shown by Greze et al. (2010) that the effect of temperature is to decrease the stress gradient in the cup wall, because of which the springback opening of the ring cut from the deep drawn cup decreases. The significant decrease of springback at 773 K for high-strength steel is caused by the increase of high-temperature creep strain just after loading process, resulting in springback reduction. It is also confirmed that the change in flow stress and Young's modulus at elevated temperatures plays a minor role in springback reduction. The study of Wang et al. (2013) reveals that the springback of AZ31B Mg alloy decreased with increase of forming temperature and decrease of punch radii during V-bending.

The study of Wang et al. (2004) and Lim et al. (2012) revealed that the time at which springback is measured also influences the accuracy of springback evaluation, and hence, the controlling and compensating strategies depend on this. A study of time-dependent springback on Al alloys such as 2008-T4, 5182-O, 6022-T4 and 6111-T4, after draw-bend tests was performed by Wang et al. It is demonstrated that the springback is proportional to log (time) up to few months, in a span of 15 months, after which no effect was observed. The creep driven by residual stress and anelasticity is proposed to be responsible for time-dependent springback. But finally, it was concluded that anelasticity is improbable to play large role in long-term time-dependent springback, but it can contribute to short-term response. Later, the workdone by Lim et al. (2012) showed that advanced high-strength steels (AHSS) such as dual-phase (DP) steel, transformation induced plasticity (TRIP) steel and conventional steels also show time-dependent springback. It was even shown that the springback found in AHSS is approximately 1/3rd of that for aluminium alloys mentioned in Wang et al. (2004) work.

In the case of tailor-welded sheets made by FSW, the selection of welding and tool conditions decides the final mechanical properties and weld microstructures and hence the overall forming performance. In this context, Park et al. (2008) have shown through unconstrained bending tests that in the case of FSW sheets made of 5052-H32 of 1.5 mm thickness, with increase in friction-stir pin diameter from 5 to 10 mm, the springback have reduced by about  $3^{\circ}$ – $5^{\circ}$ , when the weld zone (WZ) is placed longitudinally. Similarly, about  $4^{\circ}$  decrease in springback was found in the case of transverse weld, with respect to base material. The springback tests such as the unconstrained cylindrical bending, 2D draw bending and draw-bend tests were simulated by using the combined isotropic–kinematic hardening law based on the modified Chaboche model and Yld2000-2d yield function, and the predictions agree reasonably well with the experimental results (Kim et al. 2011). The work of Miles et al. (2006) also highlights the importance of friction-stir process in increasing the bending limit of welded plates made of 6061-T6 and 7075-T7451. Though the failure models that are used during finite element analysis predicted the necking limits accurately in the case of unprocessed 6061 Al plate, their prediction for friction-stir processed plate was moderately accurate. The prediction accuracy has improved once the gradient of mechanical properties in through thickness direction was captured properly by the stress–strain behaviour. Chang et al. (2002) investigated the springback characteristics of tailor-welded strips of dissimilar thicknesses made by laser welding during U-bending. The springback encountered by longitudinally welded strip was same as that of un-welded base sheets. In the case of the transverse welded strips, a significant reduction of the springback was observed in the thinner side compared with the same thickness of un-welded strip.

Ramulu et al. (2013a) analysed the effect of welding speed, rotation speed, plunge depth and shoulder diameter on the formation of internal defects, axial force and torque during FSW of 6061T6 sheets. At higher welding speed, higher rotation speed and higher plunge depth, internal defect-free weld joints are produced. The axial force and torque were not constant, and a large variation was seen with respect to FSW parameters that produced defective welds. In the case of defect-free welds, the axial force and torque were relatively constant. Recently, Ramulu et al. (2013b) studied about the effect of the welding speed and tool rotation speed on the forming limit of FS welded sheets made of AA6061-T6 with thickness of 2.1 mm using limit dome height test. With weld oriented along major straining direction, the results showed that the formability has improved by decreasing welding speed and increasing tool rotation speed. Moreover, the forming limits of FSW sheets are better than that of un-welded base materials. The strain hardening exponent of weld ( $n$ ) increases with increase in tool rotation speed and it decreases with increase in feed rate. Lee et al. (2009) evaluated the formability of FSW sheets in longitudinal weld direction, using numerical simulation and experiments. FSW sheets made of 6111-T4, 5083-H18, 5083-O, dual-phase steel (DP590) and AZ31 magnesium alloy were considered. It is observed that the improved ductility of the weld promoted the formability performance of AA5083-H18, AA5083-O and AZ31 TWB sheets. Zadpoor et al. (2008, 2009) studied the effects of the employment of the weld details on the accuracy of the failure prediction of FSW blanks, for the limiting

dome height (LDH) test and S-rail. The Marciniak–Kuczynski theory is used for the prediction of forming limits diagrams of the different zones of the FSW blanks. The WZ was modelled as a double zone, i.e. WZ and heat affected zone (HAZ) considered separately and finally recommended that implementation of the nugget zone properties is sufficient for reasonably accurate predictions of the springback behaviour.

The major objectives of the present work are (i) demonstrating the possibilities of controlling the springback of Aluminium alloys by FSW, (ii) studying the impact of a few chosen welding parameters on the springback and formability of FSW sheets and (iii) prediction of springback of FSW sheets using finite element simulations. A brief discussion has been made on the influence of few FSW parameters on the temperature evolution. A dissimilar aluminium grade combination (Al6061T6-Al5052H32) is used for springback and formability evaluation, while similar aluminium grade combination (Al6061T6-Al6061T6) is used for temperature measurement.

## 2 Methodology

### 2.1 Temperature Measurement

The base material used for temperature measurement is AA6061-T6 alloy with 2.1 mm thickness, i.e. a similar Al grade combination. The nominal chemical composition (in weight percentage) of the base material is Si: 0.65, Fe: 0.3, Cu: 0.27, Mn: 0.02, Mg: 1.0, Cr: 0.17, Zn: 0.04, Ti: 0.02 and Al: remaining. The friction-stir welding was carried out on a machine designed and developed by IISc and ETA Technologies. The process parameters varied were tool rotational speed, welding speed, plunge depth and shoulder diameter, while the tool tilt angle was kept constant at 25 °C throughout the temperature measurement. Three types of tools with flat shoulder having different diameters, and pin with equal lengths were used. These three tools were made of hot die steel with shoulder diameter 12, 15 and 18 mm, pin of frustum shape with base diameter 6 mm and top diameter 4 mm and length 1.7 mm. The welding trials were conducted at two levels of chosen parameters (Table 1) (Ramulu et al. 2013a). A third level was also selected with 15 mm shoulder diameter, at plunge depth of 1.95 mm, welding speed of 120 mm/min and tool rotation speed of 1500 rpm.

**Table 1** Optimum range of process parameters for FSW without defect formation

Shoulder diameter (mm)	Plunge depth (mm)	Tool rotation speed (rpm)	Welding speed (mm/min)
12, 18	1.85, 1.9	1300, 1400	90, 100
15	1.95	1500	120

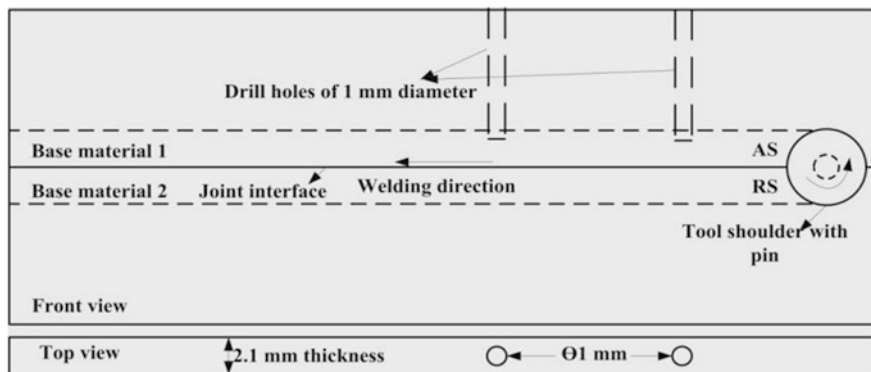


**Fig. 2** Schematic of FSW process for measuring temperature; Here, AS advancing side; RS retreating side

The drill holes were made using a conventional high-speed drilling machine with 1-mm diameter tool bit. The location of drill holes were decided by the linear interpolation of parameters for different tools as shown schematically in Fig. 2. Temperature was recorded with the help of K-type thermocouples which was inserted on end to the drilled holes of 1 mm diameter of base material in the advancing side (AS) and to the data acquisition (DAQ) system during welding. The positions of the thermocouples are such that they are 3–4 mm away from the pin for all the experiments. The temperature is recorded in the shoulder influenced region. The experimental FSW parameters for which temperature measurements were performed are tabulated in the Table 2. With tool of 12 and 18 mm shoulder diameters, three levels of experiments were performed, and with 15 mm shoulder diameter, only one experiment was performed. Temperature was recorded in all the experiments.

**Table 2** Range of FSW parameters for temperature measurement

Shoulder diameter (mm)	FSW varied parameters for experiments			Conditions for temperature measurement
	PD (mm)	RS (rpm)	WS (mm/min)	
12	1.8–1.95	1400	90	1.85 and 1.9 mm PD
	1.9	1200–1500	90	1300 and 1400 rpm RS
	1.9	1400	80–120	90 and 100 mm/min WS
18	1.8–1.95	1400	90	1.85 and 1.9 mm PD
	1.9	1200–1500	90	1300 and 1400 rpm RS
	1.9	1400	80–120	90 and 100 mm/min WS
15	1.95	1500	120	Single data

PD Plunge diameter, RS Transverse rotational speed, WS Welding speed

## 2.2 Springback Experiments and Prediction

The first step was to produce samples of friction-stir welded sheets made of Al6061T6 and Al5052H32 (a dissimilar Al grade combination) by varying the tool rotational and translational (welding) speed. The tool rotational speed was varied from 600 to 800 rpm, in three steps, and the tool translational speed was varied from 80 to 120 mm/min in three steps. AA6061T6 was placed on the AS and AA5052H32 on the retreating side (RS) of the weld during welding trials to fabricate FS welded sheets. The material properties and Lankford coefficients ( $r$ ) of the base materials (Tables 3 and 4) and weld regions (Table 5) were determined by tensile tests by using ASTM standard sub-size 1 specimen dimensions. Three trials were conducted to evaluate the tensile properties. Later, V-bending tests were performed on all the welded blanks and base materials of dimensions 160 mm  $\times$  50 mm. The weld was oriented longitudinally during bending experiments. Since time-dependent springback was reported by Wang et al. (2004) and Lim et al. (2012), the springback of all the bent sheets in the present work (included angle) were measured within an hour, after V-bending was completed. Two trials were conducted to evaluate the springback in each case. A schematic of the

**Table 3** Tensile properties of Al6061T6 base sheet

Rolling direction (degrees)	$E$ (GPa)	Yield stress (MPa)	Ultimate stress (MPa)	Uniform elongation	$n$	$K$	$r$
0	23	206	282	0.096	0.141	397.6	0.44
15	23	206	277	0.085	0.14	392.2	0.47
30	21	205	272	0.08	0.139	386.9	0.64
45	26	187	256	0.08	0.142	368.4	0.64
60	29	206	282	0.095	0.134	386.9	0.65
75	22	200	275	0.093	0.143	387.5	0.66
90	22	196	276	0.093	0.148	395.1	0.66

$E$  Elastic modulus,  $K$  Strength coefficient,  $n$  Strain hardening exponent and  $r$  Plastic strain ratio

**Table 4** Tensile properties of Al5052H32 base sheet

Rolling direction (degrees)	$E$ (GPa)	Yield stress (MPa)	Ultimate stress (MPa)	Uniform elongation	$n$	$K$	$r$
0	23	128	232	0.132	0.26	408.1	0.53
15	26	130	226	0.12	0.192	344.4	0.98
30	24	129	225	0.139	0.453	600.5	0.58
45	24	129	217	0.116	0.185	326.9	0.45
60	25	131	218	0.116	0.184	326.5	0.4
75	24	131	220	0.115	0.187	330.7	0.43
90	24	133	224	0.114	0.189	335.7	0.87

**Table 5** Tensile properties of weld region

Rotational speed (rpm)	Translational speed (mm/min)	$E$ (GPa)	Yield stress (MPa)	Ultimate stress (MPa)	Uniform elongation	$n$	$K$	$r$
600	80	29.9	110	226.3	0.167	0.211	324	0.49
600	120	30.1	100.9	226.3	0.167	0.260	359	1.68
700	80	25.5	105.3	235.3	0.181	0.255	363	0.36
700	100	30.4	113.8	252.5	0.191	0.249	380	0.54
700	120	27.5	104.6	236.4	0.175	0.256	369	0.21
800	80	30.2	104.6	245.2	0.190	0.256	374	1.11
800	100	28.8	103.9	246.5	0.186	0.259	368	0.86
800	120	26.1	86.5	217.8	0.196	0.274	340	0.73

V-bending set-up that was fabricated to conduct the experimental trials is shown in Fig. 3.

In order to predict the springback, finite element simulations were performed for V-bending (using the dimensions of setup in Fig. 3) of friction-stir welded sheets using a commercially available elasto-plastic, explicit dynamic finite element code. The adaptive meshing that automatically refines the mesh was used for finite element simulations. The meshing was done with quadrilateral shell elements of the Belytschko–Tsay formulation. Five through thickness integration points were used during simulation. The average mesh size of about 2 mm was used throughout the sheet specimen and tools. The tools were modelled as rigid bodies. The base materials properties and WZ properties obtained from experiments were incorporated during FE simulations. Hollomon’s strain hardening law was used to describe the stress–strain behaviour of base material and WZ. Hill’s 1990 yield criterion was used as the plasticity model. The ‘ $m$ ’ value used in the yield criterion was optimized to have less springback error with experimental values. The sheets were subjected to springback explicit analysis, after bending, and springback angle was evaluated. The different stages of V-bending of friction-stir welded sheets during simulations are shown in Fig. 4.

### 2.3 Formability Testing of Friction-Stir Welded Sheets

In order to evaluate the influence of shoulder diameter, rotational speed and welding speed on the formability, LDH tests were performed on the FS welded sheets made of dissimilar aluminium grade combination made of Al6061T6 and Al5052H32. AA6061T6 was placed on the AS and AA5052H32 on the RS of the weld during welding trials. The base materials properties are given in Tables 1 and 2. Standard LDH test tool geometry was used for the formability tests. Few different sheet widths (like 100 × 300 mm, 125 × 300 mm etc.) with two lubrication (dry, grease) conditions simulating four different predefined strain-paths in stretching side were



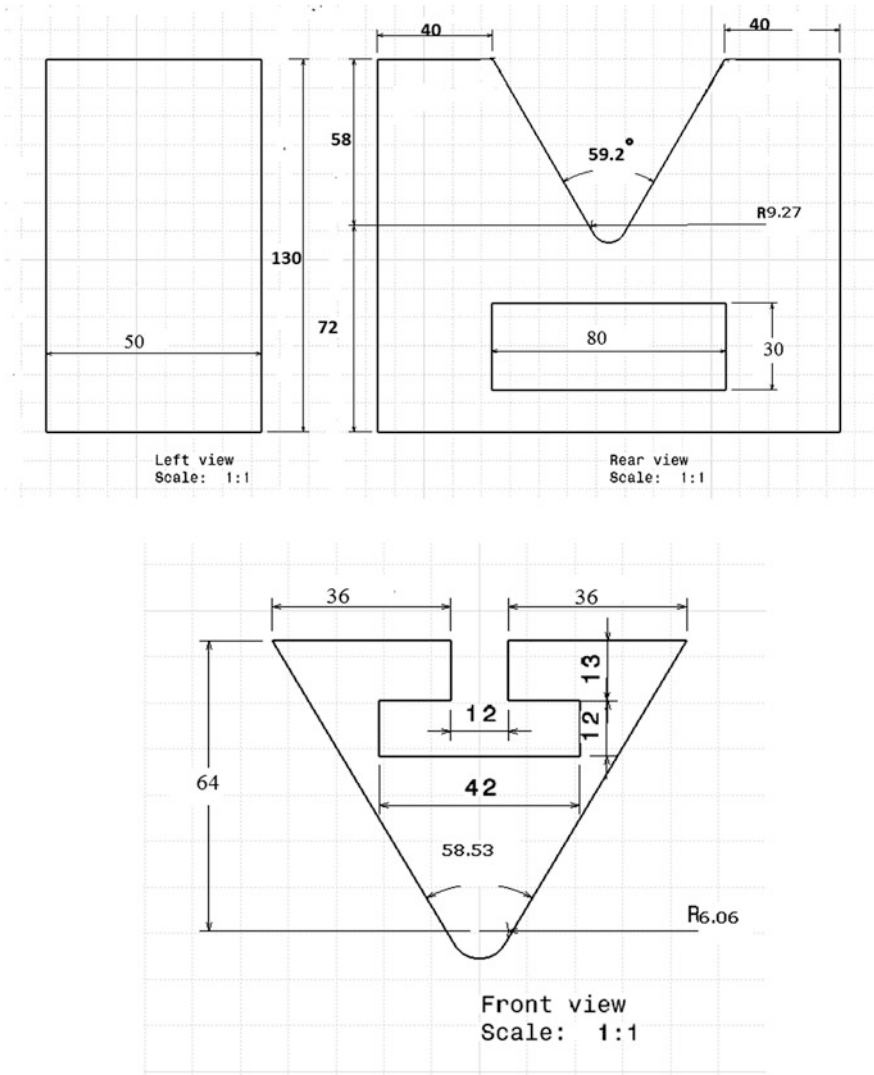


**Fig. 3** Schematic of die and punch in V-bending set-up

deformed to construct a Forming limit curve (FLC). During the LDH test, samples were first thoroughly cleaned with acetone to remove oil and dust particles on the sheet surface. The deformation of the welded sheets was analysed through the online monitoring system using spackle pattern. The pixel size in the spackle pattern was fixed at  $15 \times 6$  with a 0.6 deviation before deformation of FSW sheets. The samples were placed on the die surface with sufficient blank holding pressure. All the sheets were deformed until failure (or necking) occurs. The true major

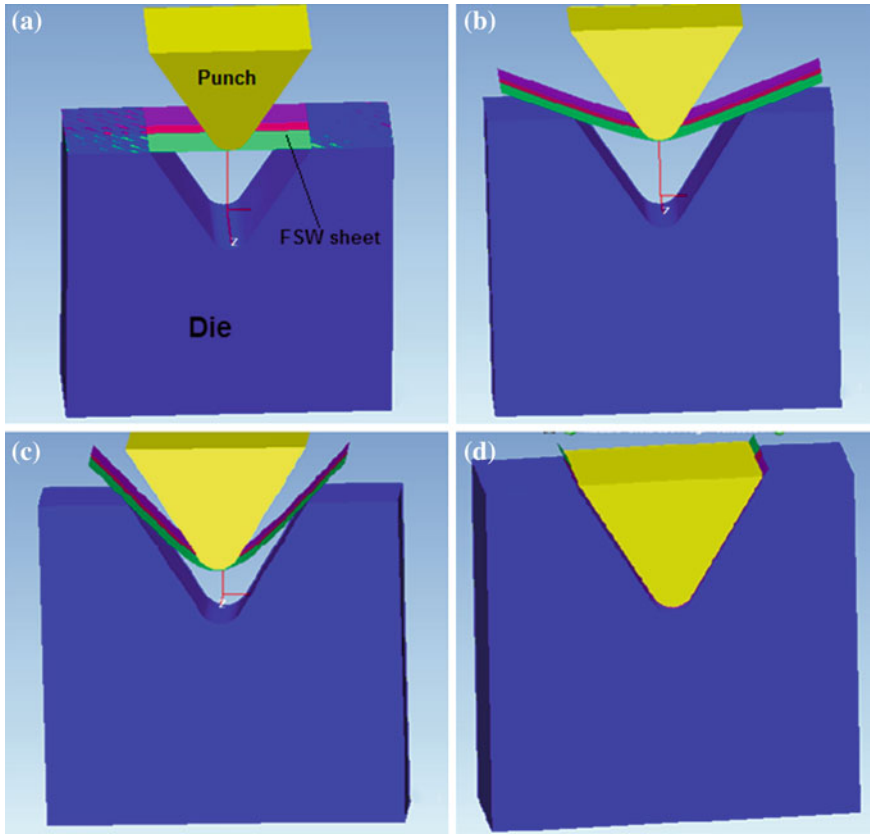


**Fig. 4** Stages of V-bending of friction-stir welded sheet during finite element simulations

strains and true minor strains near the failure and away from the failure were measured. These failure strain data were plotted on a major strain (Y-axis), minor strain (X-axis) graph. All the failed strains and safe strains were incorporated in the same graph. The FLCs were plotted such that they separate all the failed strains from the safe strains.

### 3 Results and Discussion

#### 3.1 Temperature Evolution

The influence of plunge depth, rotational speed, welding speed and shoulder diameter on the temperature evolution is described in the present section. Figures 5 and 6 show the temperature evolution at plunge depths of 1.85 and 1.9 mm, for

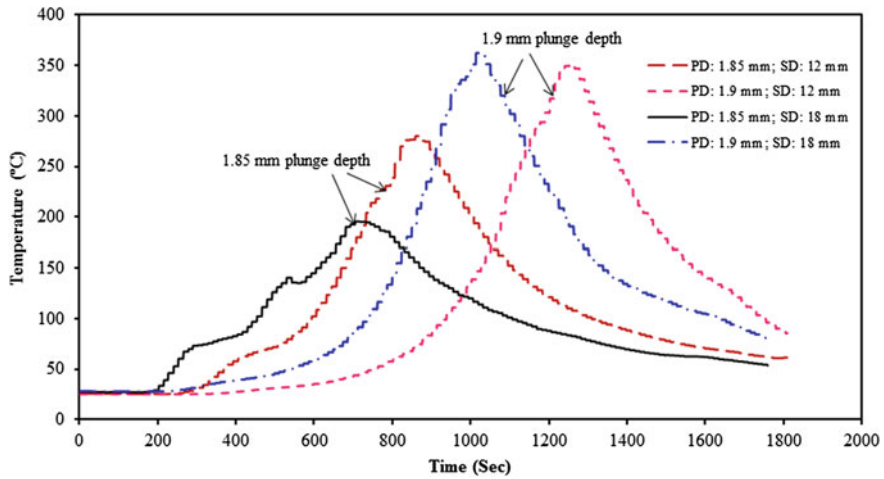


**Fig. 5** Influence of plunge depth on the temperature evolution (rotational speed: 1400 rpm, welding speed: 90 mm/min)

shoulder diameters of 12 and 18 mm, at a tool rotational speed of 1400 rpm and 90 mm/min welding speed. It is observed that the peak temperature at 1.9 mm plunge depth is more than at the 1.85 mm irrespective of the tool shoulder diameter. The peak temperatures at 1.85 mm plunge depth are 280 and 195 °C for 12 and 18 mm shoulder diameter, respectively, whereas at 1.9 mm plunge depth, 352 and 362 °C are recorded.

Similarly by increasing the tool rotational speed from 1300 to 1400 rpm, the peak temperature has increased (Fig. 6). The peak temperatures measured are 205

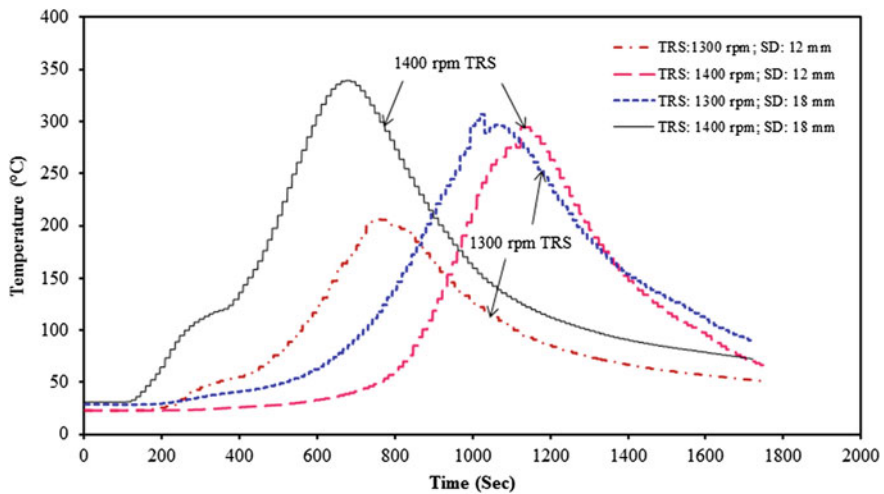


**Fig. 6** Influence of rotational speed on the temperature evolution (welding speed: 90 mm/min)

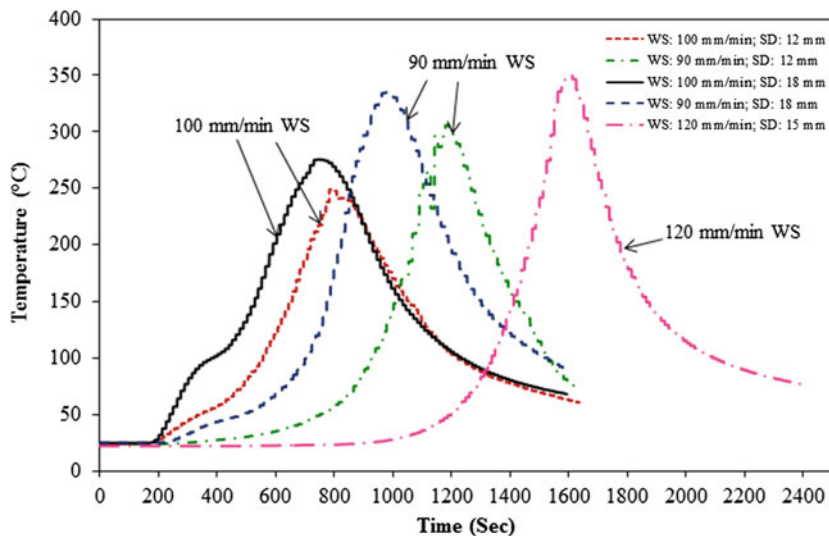


Fig. 7 Influence of welding speed on the temperature evolution

and 307 °C, at 1300 and 1400 rpm tool rotational speed, respectively. In the other case with 18 mm tool shoulder diameter at 1.9 mm plunge depth and 90 mm/min welding speed, the peak temperatures recorded are 295 and 340 °C for 1300–1400 rpm, respectively.

In case of welding speed, the peak temperature is decreased while increasing the welding speed from 90 to 100 mm/min, irrespective of tool shoulder diameter and other parameters. In the case of 12 mm shoulder diameter at 1400 rpm rotational speed and 1.9 mm plunge depth, temperature at 90 mm/min welding speed is 306 °C, and it is 249 °C at 100 mm/min welding speed (Fig. 7). Similarly in the case of 18 mm shoulder diameter, peak temperatures of 335 and 275 °C are seen at 90 and 100 mm/min welding speeds, respectively. For the third level with 120 mm/min welding speed and 15 mm shoulder diameter, the peak temperature recorded is 350 °C. The summary of peak temperature measured for different FSW combinations is given in Table 6.

The overall observation from these temperature measurements are, by increasing the shoulder diameter, plunge depth, tool rotational speed, the peak temperature has increased, while opposite behaviour is seen for welding speed. The shoulder diameter effect is due to the increase in higher temperature region, increasing the peak temperature. The plunge depth influence is due to the forging action of shoulder onto the sheet surface increasing the peak temperature. At high rotational speed, the relative velocity between the tool and sheet is high, and as a result, the heat generation rate and the peak temperature are also high. Finally at higher welding speeds, the heat input per unit length declines and at the same time, heat is dissipated over a wide region of the sheet, reducing the peak temperature.

**Table 6** Summary of peak temperature measured for different FSW combinations

FSW parameters				Peak temperature (°C)
SD (mm)	RS (rpm)	WS (mm/min)	PD (mm)	
12	1400	90	1.85	280
12	1400	90	1.9	352
12	1300	90	1.9	205
12	1400	90	1.9	295
12	1400	90	1.9	305
12	1400	100	1.9	249
18	1400	90	1.85	195
18	1400	90	1.9	362
18	1300	90	1.9	307
18	1400	90	1.9	340
18	1400	100	1.9	275
15	1500	120	1.95	350

### 3.2 SpringBack Evaluation and Prediction

The tensile behaviour of the WZ for different rotational speeds, at a constant translational speed, and for different translational speeds, at a constant rotational speed is shown in Figs. 8 and 9, respectively. It is evident that the weld properties such as yield strength, ultimate tensile strength decreases with the increase in welding speed, at a constant rotational speed of 800 rpm. There is some improvement in the ductility of the WZ with increase in welding speed and rotational speed

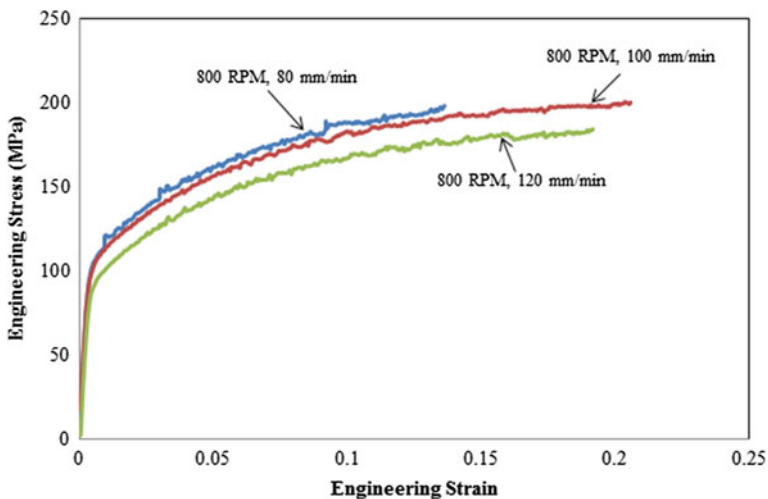


**Fig. 8** Tensile behaviour of WZ at different welding speeds

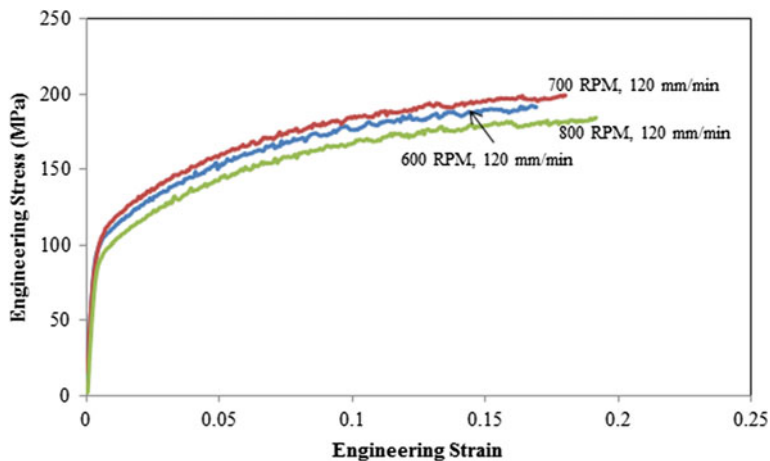


**Fig. 9** Tensile behaviour of WZ at different rotational speeds

(Figs. 8 and 9). This improvement is due to the improvement in strain hardening exponent of WZ (Table 5), improving the overall ductility of the FSW sheets. As the rotational speed increases or the welding speed reduces, the temperature in the stirring zone is expected to increase. This means that the final grain size would be larger, and it is also expected that the dislocation density reduces as the temperature increases. This leads to more static recrystallization in the WZ. It is known that the strain hardening behaviour is typically related to the accumulation and interaction of the dislocations. If the dislocation density is lower, more strain can be brought into the material, thus increasing the ductility, and finally, its forming limit has improved. In contrast, in the base material, the saturation of the dislocation density results in the lower strain hardening exponent and poor ductility, resulting in less formability. The effect of strain hardening exponent of HAZ is not considered for discussion, and hence, WZ is nothing but the nugget zone and thermo-mechanically affected zone. The relationship between strain hardening exponent of WZ and the dislocation density has been analysed by Woo et al. (2008) for a 6061-T6 Aluminium alloy, and it has been demonstrated that the low initial dislocation density in the recrystallized region is the main reason of the high strain hardening in the nugget zone.

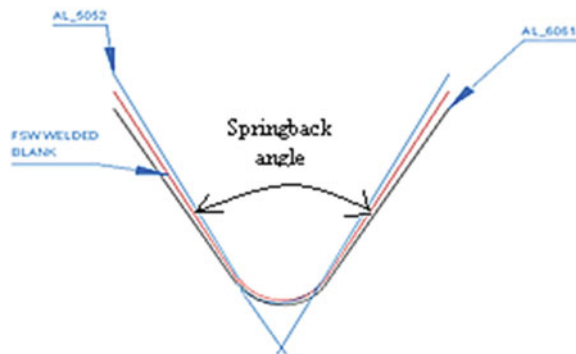
The results obtained after performing V-bending on base material sheets and welded sheets are tabulated in Tables 7 and 8, respectively. It is evident that the springback of Al5052 base material is less than that of all the welded sheets, which is lesser than the springback of Al6061 base sheets. This is shown schematically in Fig. 10.

**Table 7** Springback of base materials

Springback angle (°)	
Al6061T6	Al5052H32
64.77	56.85

**Table 8** Springback of friction-stir welded sheets

Rotational speed (rpm)	Translational speed (mm/min)	Springback (°)
600	80	62.86
700	80	58.97
800	80	60.46
600	100	63.10
700	100	62.32
800	100	61.05
600	120	61.52
700	120	60.64
800	120	59.95

**Fig. 10** Representation of relative springback of base materials and welded sheets

The influence of friction-stir welding on the springback is due to the change in WZ mechanical properties as compared to that of base materials. Two important mechanical properties, yield strength to Young's modulus ratio and strain hardening exponent, of WZ are evaluated for varied FSW conditions given in Table 5. Because of the change in rotational speed and welding speed, there is a significant change in yield stress to Young's modulus ratio ( $\sigma_y/E$ ) and strain hardening exponent ( $n$ ) of weld and this affects the overall springback of the welded sheets. Theoretically, it is known that the springback increases with the increase of  $\sigma_y/E$  ratio and decreases with  $n$  value. The influence of rotational speed and welding speed on  $\sigma_y/E$  ratio, strain hardening exponent of WZ and springback of welded sheets are shown in Figs. 11, 12 and 13.

It is observed that springback decreases with increase in rotational speed and welding speed. With increase in rotational speed,  $\sigma_y/E$  ratio of WZ decreases and ' $n$ ' value of WZ increases, decreasing the springback. At the same time, for increasing welding speed from 80 to 120 mm/min,  $\sigma_y/E$  ratio of WZ decreases and ' $n$ ' value of WZ increases, decreasing the springback of FSW sheets.

While predicting the springback, as the materials used are aluminium alloys, the yield criterion used is Hill's 1990, and the Hill's non-quadratic yield parameter ' $M$ '

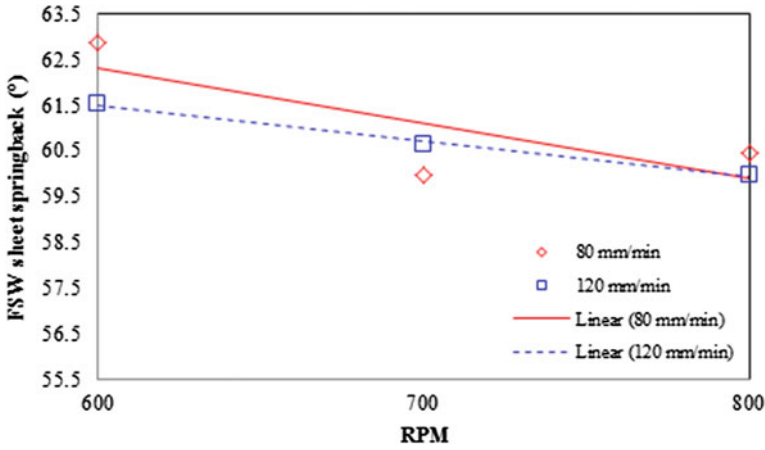


Fig. 11 Effect of rotational speed and welding speed on springback of FSW sheets (error in angle: 1.2°)

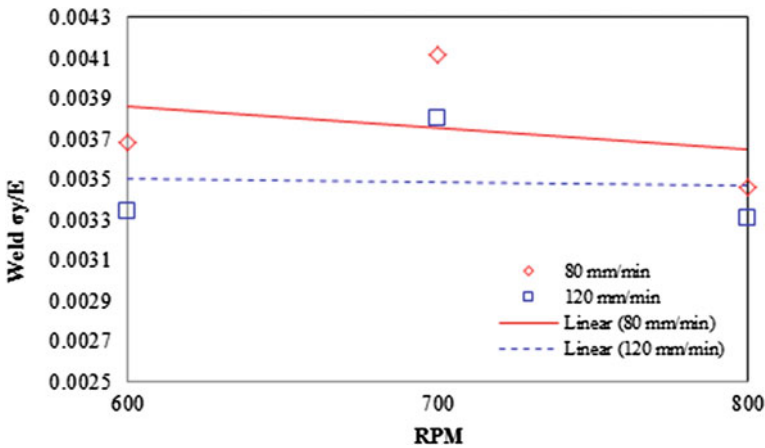


Fig. 12 Effect of rotational speed and welding speed on  $\sigma_y/E$  ratio of WZ (error in  $\sigma_y/E$ : 0.0001)

in the yield function is optimized such that for different  $M$  values between 1 and 3, the predicted and experimentally evaluated springback angles of base sheets and FSW sheets are compared (Table 9). This parameter can be evaluated through few different experimental methods including balanced biaxial stretch test and through thickness compression tests (Mulder et al. 2012). For Hill’s 1990 yield criterion, the inputs given to base material are as follows: yield strength and plastic strain ratios in seven different rolling directions, 0°, 15°, 30°, 45°, 75° and 90°, whereas for WZ, only one yield strength and plastic strain ratio are given corresponding to varied FSW conditions.



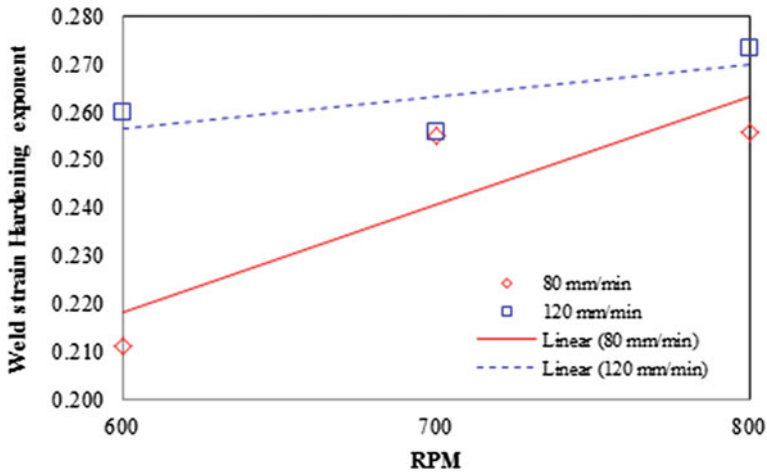


Fig. 13 Effect of rotational speed and welding speed on WZ 'n' value (error in  $n$ : 0.002)

**Table 9** Optimization of  $M$  value in Hill's 1990 yield criterion

$M$	Al6061T6 ( $^{\circ}$ )	Al5052H32 ( $^{\circ}$ )
1.8	63.04	56.24
1.9	63.56	56.43
<b>2</b>	<b>64.45</b>	<b>56.48</b>
2.1	64.22	56.25
2.2	64.23	55.85
2.3	64.18	55.92

It is observed that the springback values obtained at  $M = 2$  closely agree with the experimental springback values of  $64.77^{\circ}$  and  $56.85^{\circ}$  for Al6061T6 and Al5052H32 base sheets, respectively. Hence,  $M = 2$  was incorporated during FE simulations. The base sheets are considered as anisotropic material, and hence, plastic strain ratios given in Tables 1 and 2 are utilized. The weld region is a mix of two aluminium alloys,; therefore, simulations were performed twice, once by using the plastic strain ratios ( $r$ ) obtained experimentally (from Table 3), indicating the WZ to be anisotropic, and other by assuming that the weld region as isotropic, i.e.  $r = 1$ . The values of springback found experimentally, and those predicted by simulations are closely agreeing with each other (Table 10). The overall error between the predictions and the experimental value is 2.33 and 2.26 % in case isotropic and anisotropic WZ assumptions, respectively. Therefore, the assumption of isotropic WZ for springback predictions is acceptable for springback predictions, though anisotropic assumption will yield accurate results. Some of the bent FS welded samples are shown in Fig. 14.

**Table 10** Comparison of experimental and predicted springback values of FSW sheets

Rotational speed (rpm)	Translational speed (mm/min)	Experimental springback (°)	From simulation (assuming isotropic weld) (°)	From simulation (assuming anisotropic weld) (°)
600	80	62.86	60.13	60.70
600	120	61.52	59.77	60.08
700	80	58.97	59.54	60.26
700	100	62.32	59.97	59.98
700	120	60.64	60.04	59.49
800	80	60.46	59.72	60.27
800	100	61.05	59.18	59.09
800	120	59.95	59.10	59.40

**Fig. 14** Parent friction-stir welded sheet and bent samples

### 3.3 Formability Evaluation

The LDH tests were conducted to evaluate the forming limit of friction-stir welded sheets made of dissimilar aluminium alloy sheets under two different strain-paths and at different friction conditions (or lubrication). The sheets are formed till failure occurs, and limit strains are measured as described earlier. With this measured strain data, FLC are drawn for FSW sheets at different welding conditions to study their influence. The failure pattern of all the FSW sheets at two different strain-paths—100 (width)  $\times$  200 (length) mm (near plane-strain) and 125  $\times$  200 mm (one of the stretching strain-paths) is given in Table 11. The FSW sheets failed under three different modes: (i) failure normal to the WZ, (ii) failure along the WZ, but on the AS, and (iii) failure along the WZ, but at the centre, as shown in Fig. 15a, b (Durga Rao and Narayanan 2014). The first failure mode is seen predominantly in the case

**Table 11** Summary of failure patterns during formability testing of FSW sheets

Condition	FSW parameters			Failure pattern	
	SD (mm)	TRS (rpm)	WS (mm/min)	100 × 200 mm strain path	125 × 200 mm strain path
1	12	600	80	Pattern 1	Pattern 2
2	12	600	100	Pattern 1; draw bead failure	Pattern 2
3	12	600	120	Pattern 1	Pattern 2
4	12	700	80	Pattern 1	Pattern 2
5	12	700	100	Pattern 1; draw bead failure	Pattern 2
6	12	700	120	Pattern 1	Pattern 2
7	12	800	80	Pattern 1; draw bead failure	Pattern 2
8	12	800	100	Pattern 1	Pattern 2
9	12	800	120	Pattern 1	Pattern 2
10	16	600	80	Pattern 1; draw bead failure	Pattern 2
11	16	600	100	Pattern 1; draw bead failure	Pattern 2
12	16	600	120	Pattern 1	Pattern 3
13	16	700	80	Pattern 1; draw bead failure	Pattern 2
14	16	700	100	Pattern 1	Pattern 2
15	16	700	120	Pattern 1; draw bead failure	Pattern 2
16	16	800	80	Pattern 1	Pattern 2
17	16	800	100	Pattern 1	Pattern 2
18	16	800	120	Pattern 1	Pattern 2
19	18	600	80	Pattern 1; draw bead failure	Pattern 3
20	18	600	100	Pattern 1; draw bead failure	Pattern 2
21	18	600	120	Pattern 1; draw bead failure	Pattern 2
22	18	700	80	Pattern 1	Pattern 3
23	18	700	100	Pattern 1	Pattern 3
24	18	700	120	Pattern 1	Pattern 2
25	18	800	80	Pattern 1; draw bead failure	Pattern 2
26	18	800	100	Pattern 1	Pattern 2
27	18	800	120	Pattern 1	Pattern 2

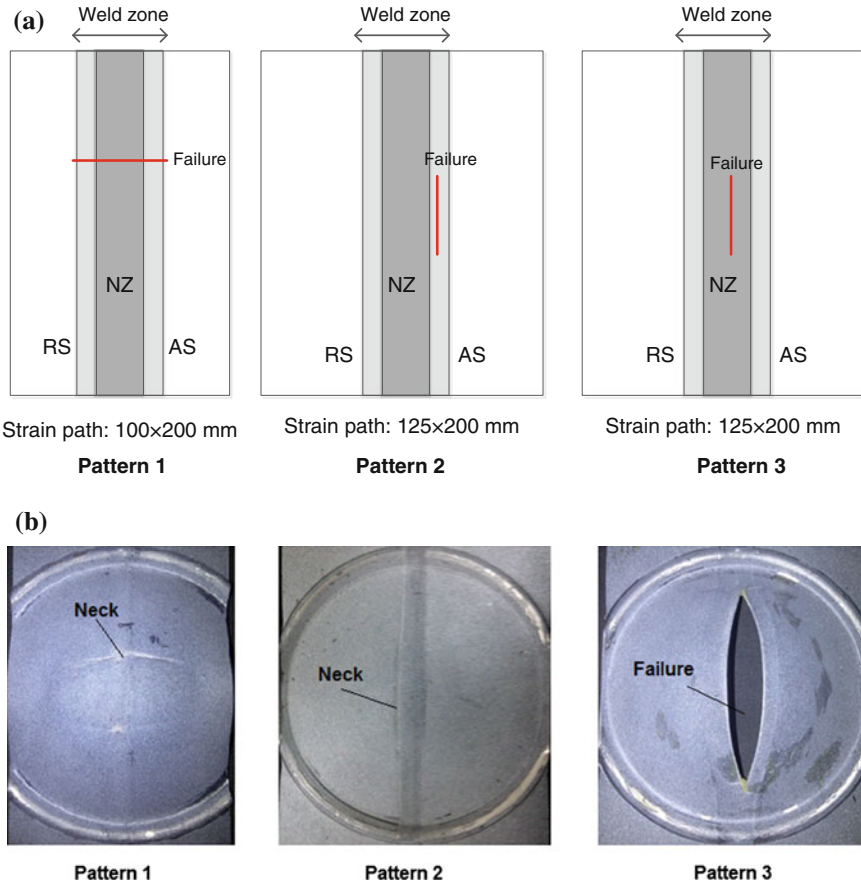


**Fig. 15** Failure pattern during LDH test of FSW sheets, **a** schematic of failure pattern at plane-strain and stretching strain-paths, **b** actual FS welded samples after failure (NZ nugget zone, AS advancing side, RS retreating side)

of plane-strain mode of deformation, i.e. for  $100 \times 200$  mm sample. Since deformation is seen only along the longitudinal and in thickness direction of the sheet, and not in width direction, the failure is expected to happen normal to the major straining direction, like in the case of simple tensile test. The second and third failure modes are seen in stretching mode of deformation, i.e. for  $125 \times 200$  mm sample. In this case, there is another pull on the width direction of the sheet, along with the longitudinal pull, making the welded sheet to fail in the weaker zone of the weld on the AS, but along the weld. In very few cases, weld failure is seen at the centre.

The forming limit diagram of FSW sheets made at two different welding conditions is shown in Fig. 16a, b. All the failed and safe strains measured during the LDH test are plotted in the same graph with true major strain in X-axis and true

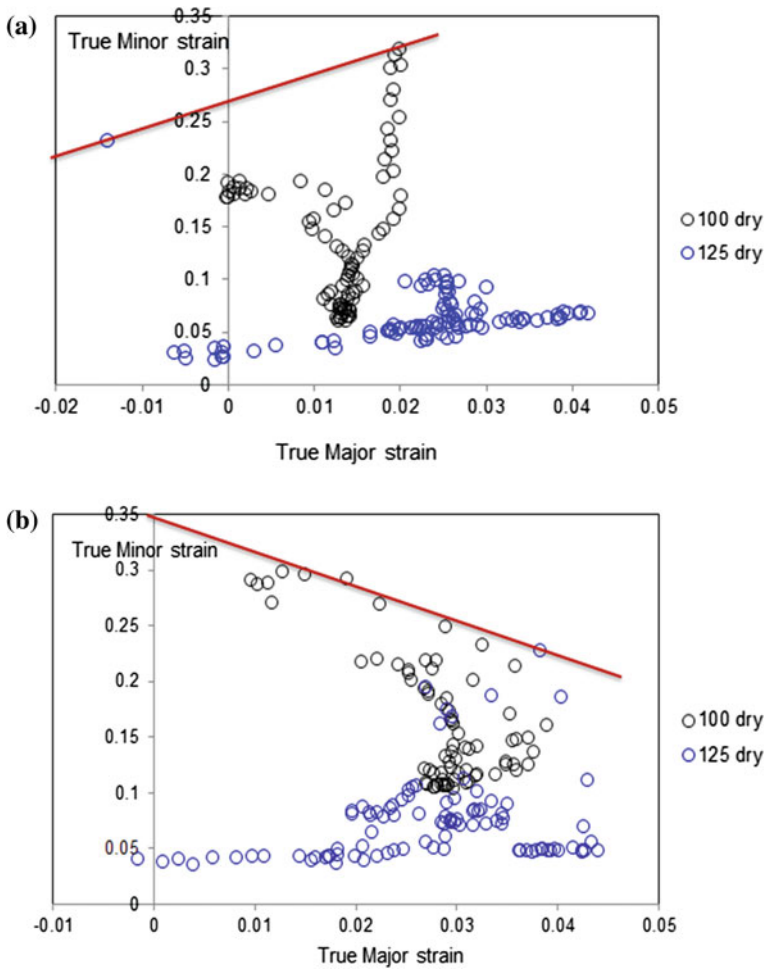


**Fig. 16** Forming limit diagram (FLD) of FSW sheets, **a** SD: 12 mm, WS: 120 mm/min, RS: 800 rpm, **b** SD: 16 mm, WS: 120 mm/min, RS: 600 rpm

minor strain in Y-axis. The largest strain defines the limit of useful formability, and hence, FLC is drawn such that all the safe strains are below the curve (Fig. 16). The same procedure is followed for all the FSW sheets, and FLC is plotted. These curves are plotted in the same graph to study the effect of FSW parameters. It should be noted from the Fig. 16b that the forming limit in the stretching side of the FLD is less than that of in plane-strain mode, i.e. FLC of FSW sheet has a negative slope, as opposed to what is generally observed in the case of un-welded sheets. This is mainly due to the change in failure pattern in the plane-strain and stretching strain-paths. In the plane-strain mode, failure occurs normal to the WZ (pattern 1),

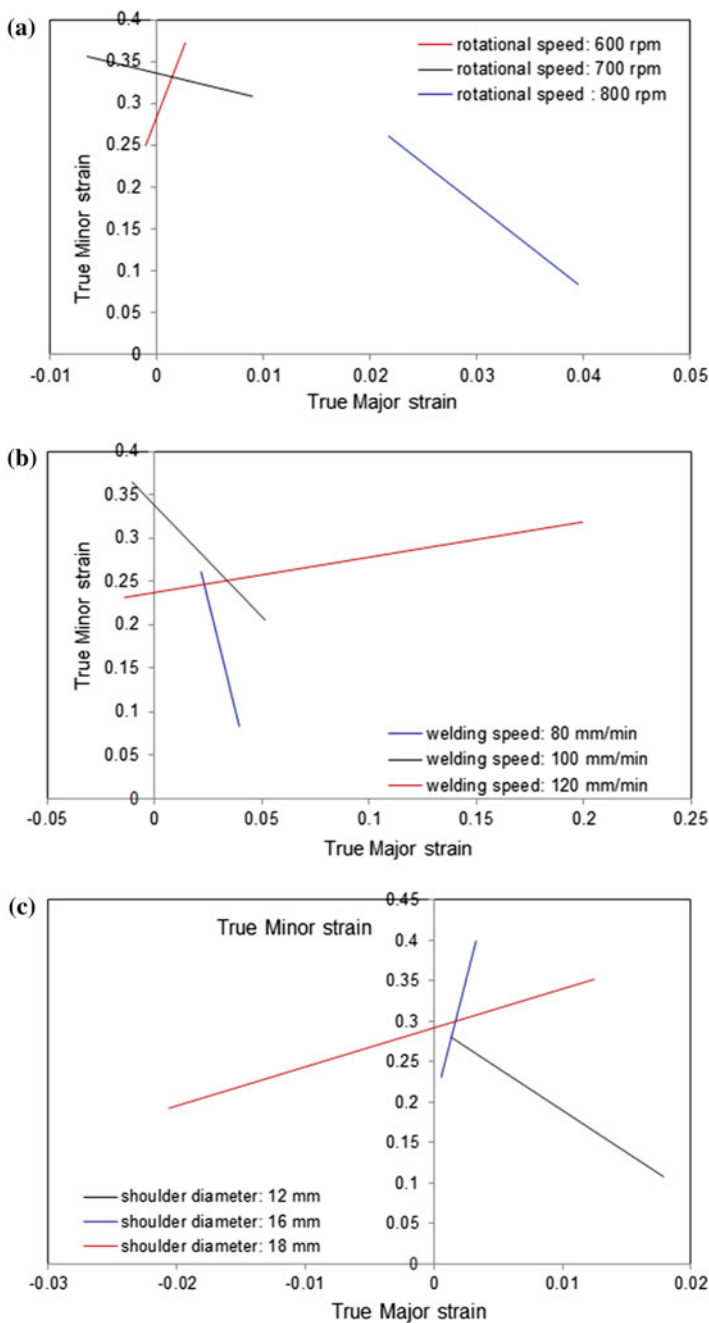


**Fig. 17** Effect of rotational speed, welding speed and shoulder diameter on the forming limit curves of FSW sheets

which has better ductility than the base material, while along the WZ in stretching mode (pattern 2 or 3), reducing the overall forming limit because of gauge effect.

The effect of rotational speed, welding speed and shoulder diameter on the FLC of FSW sheets is shown in Fig. 17a–c. It is observed that the FLC exhibit both positive and negative slopes, in an arbitrary manner, because of change in failure patterns from plane-strain to stretching mode. It has been concluded that for studying such effects on the forming limit of FSW sheets made of dissimilar grades, it is better to choose forming limit in any one of the strain-paths, either in plane-strain or tensile or stretching, rather than the whole FLC.

## 4 Conclusions

The effect of chosen FSW parameters on the temperature evolution, springback and formability of FSW sheets made of similar and dissimilar grades is studied. The following are the conclusions drawn from the present work.

1. By increasing the shoulder diameter, plunge depth and tool rotation speed, the peak temperature is increased, whereas it is decreasing for increasing welding speed. The effect of shoulder diameter is due to the increase in higher temperature region. The influence of plunge depth is due to the forging action of shoulder onto the sheet metal surface. The effect of rotational speed is due to higher relative velocity between the tool and sheet, and the influence of welding speed is due to the lower heat input per unit length and at the same time, dissipation of heat over a wider region of the sheet.
2. The ductility of WZ increases with increase in welding speed and rotational speed. This is due to the improvement in strain hardening exponent of WZ at higher rotational speed and welding speed.
3. The springback of FSW sheets is in between that of Al6061T6 and Al5052H32 base materials.
4. Reduction in springback of FSW sheets is observed at higher rotational speed and welding speed. The modifications in springback have got reasonable correlation with the modifications in  $\sigma_y/E$  ratio and  $n$  value of WZ.
5. A good correlation is observed between experimental and predicted springback values at different FSW conditions. The use of isotropic WZ assumption is acceptable during springback prediction of FSW sheets, through anisotropic WZ assumption yield slightly better results.
6. Three different modes of failures, failure normal to the WZ, failure along the WZ, but on the AS, and failure along the WZ, but at the centre, are observed during formability testing of FSW sheets made of dissimilar Al grades at two different strain-paths.

7. It is better to evaluate the forming limit of FSW sheets at individual strain-paths, rather than one full forming limit curve, because of the change in failure pattern when moved from plane-strain to stretching side. The forming limit of FSW sheets on the stretching side is lower than in plane-strain deformation mode.

**Acknowledgments** R. Ganesh Narayanan acknowledges DST, India and ARDB, India for sponsoring the projects. The present work is part of those projects.

## References

- Alves de Sousa RJ, Correia JPM, Simoes FJP, Ferreira JAF, Cardoso RPR, Gracio JJ, Barlat F (2008) Unconstrained springback behavior of Al–Mg–Si sheets for different sitting times. *Int J Mech Sci* 50:1381–1389
- Chang SH, Shin JM, Heo YM, Se DG (2002) Springback characteristics of the tailor-welded strips in U-bending. *J Mater Process Technol* 130–131:14–19
- Durga Rao B, Narayanan RG (2014) Springback of friction-stir welded sheets made of aluminium grades during V-bending: an experimental study. *ISRN Mech Eng Article ID 681910*. doi:[10.1155/2014/681910](https://doi.org/10.1155/2014/681910)
- Garcia-Romeu ML, Ciurana J, Ferrer I (2007) Springback determination of sheet metals in an air bending process based on an experimental work. *J Mater Process Technol* 191:174–177
- Greeze R, Manach PY, Laurent H, Thuillier S, Menezes LF (2010) Influence of the temperature on residual stresses and springback effect in an aluminium alloy. *Int J Mech Sci* 52:1094–1100
- Kim J, Lee W, Chung KH, Kim D, Kim C, Okamoto K, Wagoner RH, Chung K (2011) Springback evaluation of friction-stir welded TWB automotive sheets. *Met Mater Int* 17:83–98
- Lee W, Chung KH, Kim D, Kim J, Kim C, Okamoto K, Wagoner RH, Chung K (2009) Experimental and numerical study on formability of friction-stir welded TWB sheets based on hemispherical dome stretch tests. *Int J Plast* 25:1626–1654
- Lim H, Lee MG, Sung JH, Kim JH, Wagoner RH (2012) Time-dependent springback of advanced high strength steels. *Int J Plast* 29:42–59
- Miles MP, Mahoney MW, Fuller CB (2006) Prediction of bending limits in friction-stir-processed thick plate aluminum. *Metall Mater Trans A* 37A:399–404
- Mishra RS, Ma ZY (2005) Friction-stir welding and processing. *Mater Sci Eng R* 50:1–78
- Moon YH, Kang SS, Cho JR, Kim TG (2003) Effect of tool temperature on the reduction of the springback of aluminum sheets. *J Mater Process Technol* 132:365–368
- Mulder J, Vegter Henk, Jin Jin Ha, van den Boogaard AH (2012) Determination of flow curves under equibiaxial stress conditions. *Key Eng Mater* 53:504–506
- Park S, Lee CG, Kim J, Han HN, Kim SJ, Chung K (2008) Improvement of formability and springBack of AA5052-H32 sheets based on surface friction-stir method. *J Eng Mater Technol* 130: 041007-1–041007-10
- Ramulu PJ, Ganesh Narayanan R, Kailas SV, Reddy J (2013a) Internal defect and process parameter analysis during friction-stir welding of Al 6061 sheets. *The Int J Adv Manufact Technol* 65: 1515–1528
- Ramulu PJ, Kailas Satish V, Ganesh Narayanan R (2013b) Influence of tool rotation speed and feed rate on the forming limit of friction-stir welded AA6061-T6 sheets. *Proc Inst Mech Eng Part C: J Mech Eng Sci* 227:520–541
- Wang JF, Wagoner RH, Carden WD, Matlock DK, Barlat F (2004) Creep and anelasticity in the springback of aluminium. *Int J Plast* 20:2209–2232



- Wang L, Huang G, Zhang H, Wang Y, Yin L (2013) Evolution of springback and neutral layer of AZ31B magnesium alloy V-bending under warm forming conditions. *J Mater Process Technol* 213:844–850
- Woo W, Balogh L, Ungár T, Choo H, Feng Z (2008) Grain structure and dislocation density measurements in a friction-stir welded Aluminum alloy using X-ray peak profile analysis. *Mater Sci Eng A* 498:308–313
- Zadpoor AA, Sinke J, Benedictus R, Pieters R (2008) Mechanical properties and microstructure of friction-stir welded tailor-made blanks. *Mater Sci Eng A* 494:281–290
- Zadpoor AA, Sinke J, Benedictus R (2009) Finite element modeling and failure prediction of friction-stir welded blanks. *Mater Des* 30:1423–1434